*Journal of Biochemical and Biophysical Methods*, 23 (1991) 1-30

*ADONIS* 0165022X9100076M

JBBM 00883

Review

# Investigation of biological systems by high resolution 2-mm wave band ESR

V.I. Krinichnyi

*Institute of Chemical Physics, U.S.S.R. Academy of Sciences, Chernogolovka, U.S.S.R.*

(Received 20 October 1989)
(Accepted 14 February 1991)

**Summary**

The application of high resolution ESR to the investigation of various biological systems is discussed. The advantages of the technique in the study of structural, conformational and dynamic characteristics have been exemplified by spin-labeled human serum albumin, egg lysozyme, liposome membranes, inverted micelles, α-chymotrypsin, cotton fiber and cellulose. The polarity of the microenvironment and the mechanism of molecular mobility of the objects under study have been determined. The combination of high resolution and saturation transfer techniques has been shown to give a detailed analysis of very slow molecular motions in biological objects. Peroxide radicals in biosystems have been identified from their ESR spectra at the 2-mm wave band.

Key words: Spin label method; ESR spectroscopy; Biological system

## Introduction

Various methods exploiting labels or probes are widely used in investigations of the structure and dynamics of biological systems. They include luminescent labels [1], nuclear gamma-resonance (NGR) labels [2], electron scattering labels [3] and others. One of the most commonly used is the spin label or spin probe method based on the introduction of a nitroxyl radical into biological systems [4-7]. The ESR spectral parameters of radicals depend on the polarity, structure and dynamics of their microenvironment. Therefore, the introduction of spin labels or probes into various sites of enzymes, nucleic acids and membranes reveals the profiles of polarity and molecular mobility of the systems under study and their topography.

*Correspondence address:* V.I. Krinichnyi, Institute of Chemical Physics, U.S.S.R. Academy of Sciences, Chernogolovka, 142 432, U.S.S.R.

Such investigations are most commonly carried out using 3-cm wave band ESR. However, the ESR spectra of organic free radicals are registered in a narrow range of magnetic fields at this RF wave band. This leads to poor resolution of multicomponent ESR spectra and makes difficult the application of this method to the study of structure and dynamics of the microenvironment in biological systems.

For example, 3-cm wave band ESR spectra do not give an unequivocal interpretation of the factors which cause relaxation changes in the spectrum (e.g., slow anisotropic movement of radicals in the frequency range $\nu = 10^7 — 5 \cdot 10^8$ $s^{-1}$ [4] or fast rotation of a nitroxyl radical with $10^9$ $s^{-1}$ frequency within a cone [8]). Additional difficulties also arise in registering ESR spectra of some paramagnetic centers with similar magnetic parameters, as well as in determining micropolarity in biological systems [6].

Thus, the ESR study of biological systems at the 3-cm wave band faces considerable limitations.

In some specific cases an increase in accuracy may be achieved by a non-modulated ESR method [9]. Low molecular mobility in the frequency range of $\nu < 10^7$ $s^{-1}$ can be measured by the method of microwave saturation transfer (ST ESR) [5,10]. The efficiency of the 3-cm wave band technique may be increased by deuteration of the radicals or solvent medium, which lowers the contribution of their protons to the width of the spectral components [11].

However, the millimetric wave band ESR technique has proved to be a more efficient and precise method of spectra registration [12-16]. At this wave band absolute sensitivity and spectral resolution increase considerably for polyoriented paramagnetic centers in model systems.

The present article first reviews results obtained in the study of the microstructure and dynamics of a wide range of biological samples (proteins, enzymes, membranes, micelles, α-chymotrypsin, cotton fibers and cellulose) using high spectral resolution ESR at the 2-mm wave band [17]. The potential of this technique for the detailed study of very slow anisotropic movements of nitroxyl radicals by ST ESR and the identification of peroxide radicals in biological systems are discussed.

## The ESR method in the study of biological systems

The paramagnetic properties of nitroxyl radicals used as spin labels and probes result from the intrinsic magnetic moment of the unpaired electron localized on the molecular *p*-orbital (Fig. la). When the external magnetic field $H_o$ is applied to a system of such radicals, their spins are oriented along or against the field direction. These orientations differ in the value of their interaction with the magnetic field; therefore in the paramagnetic system there appear two Zeeman energy levels with different spin populations. If, besides the constant magnetic field, the spin system is also subjected to an RF field of frequency $\nu$ with a magnetic component $H_1$ perpendicular to $H_o$, then a translation will be induced from one spin state to another with the resonant absorption of RF energy. The condition for this transition is:

$$h\nu = g\beta H_0 \qquad (1)$$

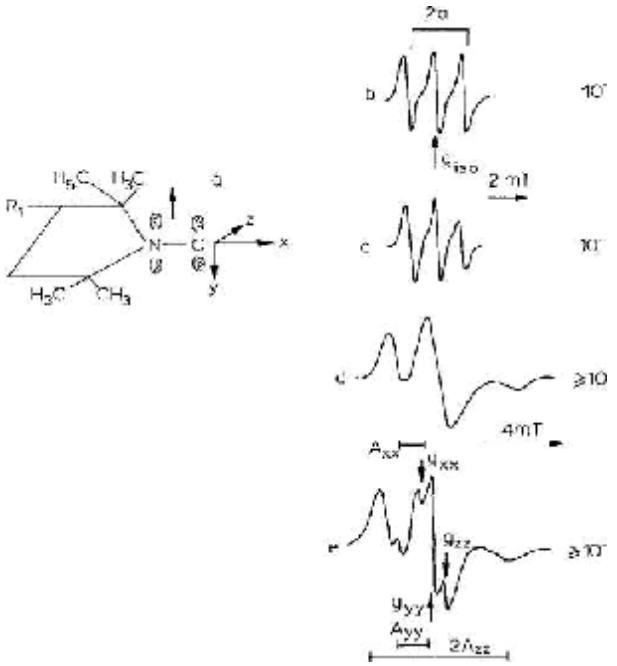


Fig. 1. Electronic configuration of the nitroxyl radical in the molecular system of coordinates *(R* is the radical substituent). (*a*): typical ESR spectra of this radical at various correlation times of rotation (*b* - *e*) and of a deuterosubstituted radical in $d_8$-toluene at 140 K (*e*) [6,50]. The measured magnetic parameters are also shown.

where $h$ is Planck's constant, $v$ is the frequency of the RF field, g is the Lande factor equal to 2.00232 for a free electron on the *s*-orbital, β is the Bohr magneton and $H_o$ is the external magnetic field strength.

Atomic orbitals of the nitroxyl radical are rigidly fixed and oriented in the molecular system of coordinates by strong atomic electric fields. In addition, the unpaired electron participates in the orbital motion around O and N heteroatoms, which produces a considerable deviation of its *g*-factor from the free electron *g*-factor and results in its dependence on the radical orientation in the magnetic field.

The differences in *g*-factor values from 2.00232 along the molecular *x*- and *y*-axes are given by [18]:

$$\Delta g_{xx} = g_e \lambda_0 \rho_O^{\pi} / \Delta E_{n\pi^*} \text{ and } \Delta g_{yy} = g_e \lambda_0 \rho_O / \Delta E_{\sigma\pi^*} \qquad (2)$$

respectively, where $g_e$ is the free electron *g*-factor; $\lambda_o$ is the constant of spin-orbital interaction with the oxygen nucleus; $\rho_O^{\pi}$ is the density of the unpaired electron on the oxygen atom; $\Delta E_{np^*}$ and $\Delta E_{\sigma\pi^*}$ are energy differences of the corresponding molecular orbit. The lowest change in the *g*-factor is observed when the magnetic field is along the *z*-axis of the radical.

The other important characteristic of nitroxyl radicals is the hyperfine interaction (HFI) between the unpaired electron and the nuclear spin ($I$=1) of the nitrogen

atom. This interaction depends on the configuration and density of the spin cloud on the nitrogen nucleus and is characterized by the *A*-tensor.

Thus, the magnetic parameters of the nitroxyl radical are affected by its orientation in the magnetic field and defined by *g*- and *A* -tensors.

In condensed media of low viscosity the components of the *g*- and *A*-tensors are averaged due to fast radical rotation. In this case the ESR spectrum of the nitroxyl radical is a triplet of equidistant lines with the same intensities; it is characterized by the isotropic magnetic parameters (Fig. lb).

$$g_{iso} = (g_{xx} + g_{yy} + g_{zz})/3 \text{ and } a = (A_{xx} + A_{yy} + A_{zz})/3 \quad (3)$$

where $g_u$ and $A_u$ are the diagonal values of *g*- and *A* -tensors, respectively. With increasing viscosity of the medium anisotropy of the radical magnetic parameters is reflected in the ESR spectra (Fig. lc-e).

The magnetic parameters are essentially affected by structural and dynamic properties of the nitroxyl radical environment.

In biological systems nitroxyl radicals can form donor-acceptor, electrostatic and other complexes with molecules in their environment [19]. About 1% of the spin density in donor-acceptor complexes is transferred to the ligand as a result of hydrogen bond formation. The magnetic constants of such a complex depend on the donor-acceptor properties of the ligand. In electrostatic complexes the interaction between dipoles of the ligand and the radical causes electrostatic perturbation of Huckel molecular orbitals and Coulomb integrals of the N-O fragments. The dipole-dipole interaction leads predominantly to changes in the $A_{zz}$ value of the HFI tensor [20], which can be determined from the following equation:

$$\delta A_{zz} = B\mu_l\rho_l M_l^{-1} \quad (4)$$

where $B = 22\, er\beta^{-1}kT\mu_r$ (*e* is the elementary charge, *r* is the N-O fragment radius, $\beta$ is the resonant integral of the C-C bond, $\kappa$ is Boltzmann's constant, *T* is the absolute temperature, $\mu_r$ is the radical dipole moment) and $\rho_l$, $M_l$ and $\mu_l$ are the effective density, molecular weight and dipole moment of the environment, respectively.

Complex formation also leads to a shift of the $n\pi^*$ band in the electron absorption spectrum of the radical, which is evidence for an energy change in the $n\pi^*$ orbital transition. Interaction of the radical with electron acceptor or electron donor ligands lowers the energy levels of *n* or $\pi^*$ orbitals, respectively, thus affecting the $g_{xx}$ value [18].

Thus, in condensed media, an increase in the polarity of the nitroxyl radical microenvironment decreases the $g_{xx}$ value and increases the $A_{zz}$ value. Unlike simple models, in biological systems radicals can form complexes with nearby hydroxyl groups of different nature. This can cause inhomogeneous broadening and sometimes splitting of the ESR spectrum into separate components.

As stated above, an increase in viscosity results in a decrease in rotation frequency of the radical, and the anisotropy of its magnetic parameters appears in

ESR spectra (Fig. 1, c-e). The theory of spectra of isotropically rotating radicals with a correlation time of $\tau_c < 10^{-9}$ s has been well developed [21-23]. At slower rotation a comparison between the experimental and computer ESR spectra is usually required. The computation algorithm and the form of the computed ESR spectra depend on the motion pattern chosen. As a rule, the mobility of spin labels and probes in biological systems is determined by various parameters of their environment and is strongly hindered. Because of the non-sphericity of routinely used radicals, their motion is generally anisotropic in the majority of biological systems. In this case the relaxation changes in the ESR spectra of randomly oriented spin-labeled systems should not appear for that fraction of radicals which are mainly oriented with the preferred rotation axis along the field.

Thus, for a radical undergoing increasing rotation about the molecular x-axis, relaxation changes will take place primarily in the *y* and z components of the ESR spectrum. As motion increases further the *x* component also becomes involved. The relaxation changes are revealed in the shift and broadening of the principal values of the ESR spectrum. The value of broadening, $\delta H_i$, is proportional to the frequency of slow ($\nu < 5 \cdot 10^8$ $s^{-1}$) radical reorientation with respect to the direction of the external magnetic field [15]:

$$\delta H_x \approx 2\nu_\perp/\gamma;\ \delta H_y = \delta H_z \approx (\nu_\perp + \nu_\parallel)/\gamma \qquad (5)$$

Where $\gamma$ is the gyromagnetic ratio, and $\nu_\parallel$ and $\nu_\perp$ are the frequencies of the radical reorientation in parallel and perpendicular orientation to the external field, respectively. These conclusions are also valid for radicals with other axes of preferred rotation.

Thus, the precise study of the structure and dynamics of biological spin-labeled systems requires the determination of all principal values of their magnetic constants.

However, the principal lines overlap almost completely in the ESR spectrum of nitroxyl radical in condensed medium measured at the 3-cm wave band (see Fig. 1d, e). Some of the components of *g*- and *A* -tensors of deuterated spin systems may be obtained from ESR spectra at the 3-cm wave band if the line width is small (Fig. le). In real biological systems the problem of magnetic parameter definition is more complicated. As a rule, only the magnetic parameters $g_{zz}$, $A_{zz}$ and the *z*-component width can be determined from 3-cm ESR spectra.

As stated above, the accuracy and resolution of the ESR spectra increase at higher RFs. However, at the 8-mm ESR wave band, the anisotropy of the *g*-factor is comparable with that of HFI so that lines of different orientation are coincident to a considerable degree [24].

At the 2-mm wave band the resolution between spectral lines increases by more than an order of magnitude [13] (Fig. 2), making it possible to determine all magnetic parameters of nitroxyl radicals. An independent analysis of relaxation changes in each component of the spectra and the study of anisotropic low molecular rotations become possible. Although the $A_{xx}$ and $A_{yy}$ values are not resolved in biological systems because of unpaired electron interaction with radical

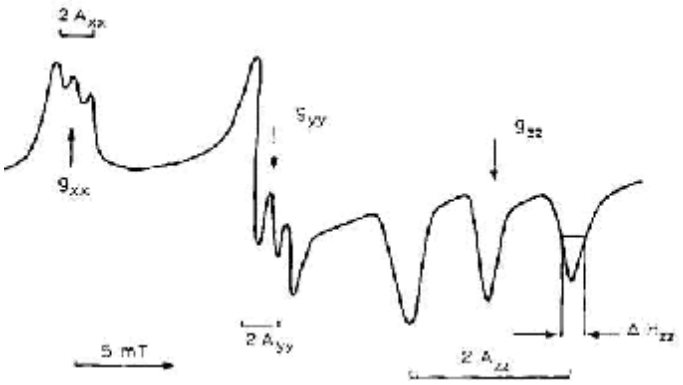


Fig. 2. The ESR spectra of the 2-mm range of the deuterosubstituted nitroxyl radical in $d_8$-toluene recorded at 140 K [50]. The measured magnetic parameters as well as standard $Mn^{2+}$-lines are shown.

protons and with the local environment, they are easily determined from the halfwidth of the corresponding canonic components.

Thus, the high spectral resolution at the 2-mm wave band of ESR makes it possible to study fine structural and conformational transitions in the native biological object. The configuration of the spin distribution in organic radicals and the detection of several radicals with similar magnetic parameters can be more successfully determined at this wave band.

**Characteristics of 2-mm ESR spectroscopy**

According to Eqn. 1, microwave radiation at the 2-mm wavelength and a strong constant magnetic field (about 5 T) are required to detect paramagnetic centers with $g \approx 2$ at the 2-mm ESR wave band. Therefore the 2-mm wave band ESR spectrometer includes an $H_{011}$ microwave cavity and a superconducting magnet [25]. A general block diagram of the 2-mm wave band ESR device is given in Fig. 3. The main part of the spectrometer includes the microwave klystron oscillator (*11*) with some elements of the waveguide section and a cryostat (*1*) with a super conducting solenoid (*2*), in whose warm channel the tunable resonator (*5*) with a sample (*6*), temperature-sensitive (*3*) and modulator (*4*) coils are inserted. The sample, contained in a thin (0.5 mm) quartz capillary (7 mm long), is placed in the center of the cavity with a mobile plunger.

The microwave cavity with the sample inside is temperature-controlled (80 — 370 K). However, the recording of the ESR spectrum at lower temperatures is not excluded.

The *Q* factor of the cavity (inner diameter 3.5 mm, operational height 1.5 mm) is equal to 2000. The value of the microwave magnetic field component is 20 μT in the center of the cavity. Inhomogeneity of the magnetic field in the sample situation did not exceed $10^{-5}$ T/mm.

The absolute point-sample sensitivity of the spectrometer is $5 \cdot 10^8$ spins/mT. The concentration sensitivity for an aqueous sample is $6 \cdot 10^{13}$ spins/mT cm$^3$. In the latter case the samples were placed in capillaries of smaller diameter to retain the high $Q$ factor.

All experiments were carried out at high frequency (100 kHz) modulation.

The g-factor calibration is performed using the $Mn^{2+}$ standard with $a$ = 8.74 mT and $g$ = 2.00102. The 2nd order correction to the effective resonant field [26] for this standard is 65 μT, which does not contribute any significant error to the determination of the magnetic constants.

**The structure of microenvironment and molecular mobility of nitroxyl radicals in biological systems**

In the ESR investigation of biological objects at the 2-mm wave band the following nitroxyl radicals were used as spin labels and probes:

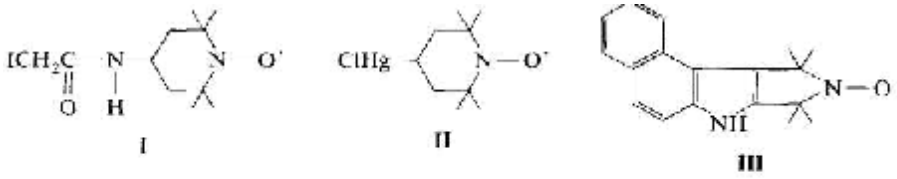

I



II



III

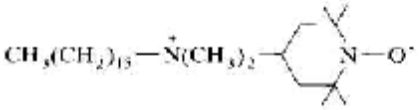

IV

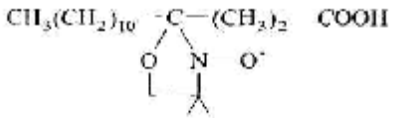

V

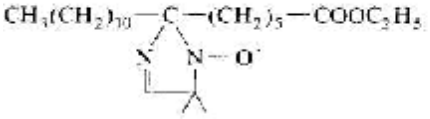

VI

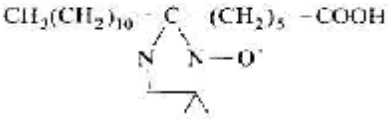

VII

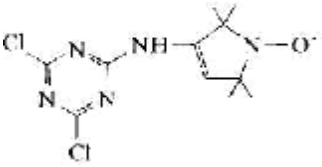

VIII

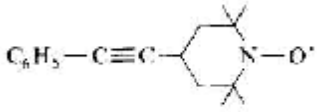

IX

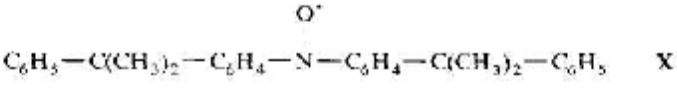

X

The magnetic constants of the spin labels and probes in various matrices were determined from their ESR spectra recorded at a temperature when all movement in the sample was frozen (see Appendix).

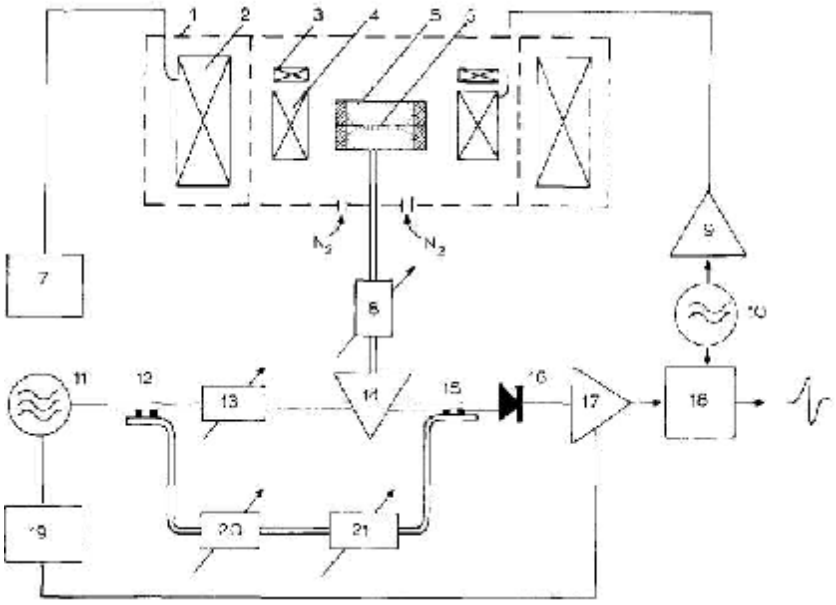


Fig. 3. Block diagram of the 2-mm wave band ESR spectrometer [25]: (*1*) helium cryostat; (*2*) superconducting solenoid; (*3*) temperature-sensitive coil; (*4*) a.c. modulator coil; (*5*) microwave cavity; (*6*) sample; (*7*) solenoid supply; (*8*) and (*21*): phase shifter; (*9*) a.c. modulator amplifier; (*10*) a.c. oscillator; (*11*) Klystron oscillator; (*12* and *15*) directional MW couplers; (*13* and *20*) MW attenuators; (*14*) MW circulator; (*16*) superlow temperature (4.2 K) barretter; (*17*) a.c. preamplifier; (*18*) ESR amplifier and synchronous detector; (*19*) section of auto adjustment of the MW klystron oscillator.

Let us consider the influence of the radical structure on its ability to form complexes with its microenvironment. Unlike the 5-member radicals, which have a flat conformation, the 6-member radicals exist predominantly in the chair form. Therefore the «-orbital of the 6-member radicals is more accessible to the environment, permitting the formation of higher energy hydrogen bonds.

In fact, the average slopes of the $g_{xx}$ — $A_{zz}$ correlation of 6- (**I**, **II**) and 5-member (**III**, **VII**, **VIII**) radicals in biological and model systems are $2.3 \cdot 10^{-3}$ $mT^{-1}$ and $1.2 \cdot 10^{-3}$ $mT^{-1}$, respectively (see Appendix). This confirms a greater shift of the spin density to the nitrogen atom when 6-member radicals form complexes with a microenvironment of the same polarity [18].

In Fig. 4 the correlation is shown between experimental changes of $A_{zz}$, $\delta A_{zz}^{exp}$, and calculated ones, $\delta A_{zz}^{calc}$, for 6-member radical **I** (o) and for 5-member radical **VII** (□) in various model systems. As may be seen from the figure, the linear dependence between the $\delta A_{zz}^{exp}$ and $\delta A_{zz}^{calc}$ values for both radicals holds only in model systems with a dipole moment not exceeding 1.7 Debye. Therefore, the presence of negligible electrostatic and donor-acceptor radical complexes with the microenvironment may be assumed for these systems. The difference in slopes indicates that 6-member radicals are more sensitive to the polarity and structure of their environment.

Thus, the simultaneous existence of different radical complexes is possible both in model and biological systems. The magnetic constants of the radical are de-

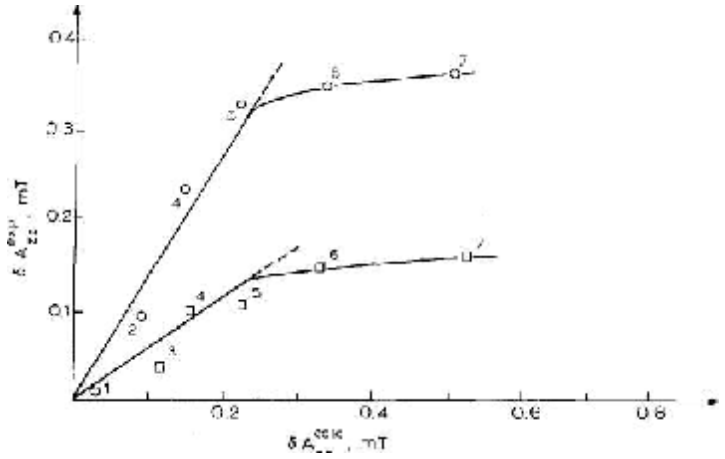


Fig. 4. The correlation plots $\delta A_{zz}^{exp}$ vs. $\delta A_{zz}^{calc}$ for radicals **I** (o) and **VII** (□) in frozen toluene (*1*), isopropanol (*2*), *n*-propanol (*3*), ethanol (*4*), methanol (*5*), water-ethanol (3:1) mixture (*6*) and water-glycerol (10:1) mixture (*7*) [17].

termined by the proportions of these complexes and the effective polarity and structure of their environment.

As shown above, the $g_{xx}$ and $A_{zz}$ values are the most sensitive to the changes in polarity and structure of the nitroxyl radical environment. Therefore, these properties are determined with the use of the correlation between these values, $g_{xx}$ — $A_{zz}$, in biological and model systems.

*Egg lysozyme.* Lysozyme samples modified by spin label **I** on His-15 group [27] were studied at 2-mm wave band ESR [28]. The ESR spectrum of the lyophylized sample is characterized by a strong inhomogeneous broadening of the canonic components. The broadening is partially decreased after sample dampening. This observation suggests that there is an interaction between nitroxyl radicals and different hydroxyl groups in the dry sample.

The magnetic constants of samples of frozen egg lysozyme and a-chymotrypsin modified by radical **I**, human serum albumin modified by radicals **I** — **III** at the same relative humidities and a solution of radical I in organic solvents of different polarities are presented in Fig. 5. As may be seen from the figure, an increase in the polarity of the microenvironment of radical **I** in model systems causes a gradual decrease in the $g_{xx}$ values but an increase in the $A_{zz}$ values. This observation provides unequivocal evidence for the formation of an *n*-σ radical complex with molecules of the medium [19]. The deviation of the experimental correlation $g_{xx}$ — $A_{zz}$ from linearity can be explained by the presence of electrostatic and donor-acceptor complexes in model systems.

A gradual change in the magnetic constants of label **I** takes place as lysozyme becomes saturated by water (see Fig. 5). Obviously, there exists an *n*-σ complex of the radical N-O moiety with its environment in modified lysozyme. The close values of the magnetic constants of the radical **I** in lyophilized protein and in butanol

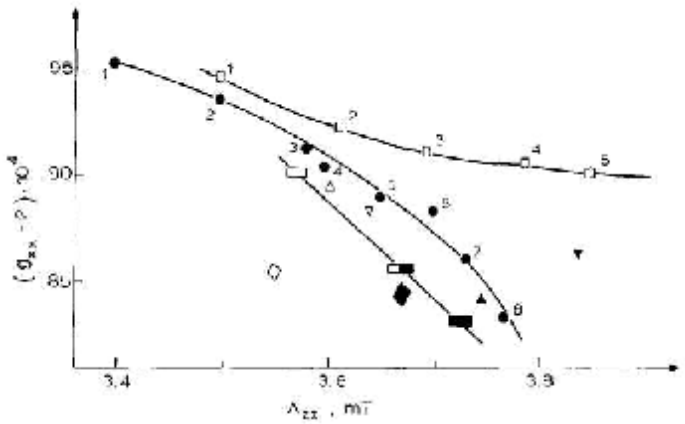


Fig. 5. The correlation plot $g_{xx}$ — $A_{zz}$ for radical **I** in frozen (140 K) ( , ) toluene (*1*), isobutanol (*2*), ethanol (3), water-ethanol mixture with 0.25 (*4*), 0.50 (*5*), 0.66 (*6*), $H_2O$ content, methanol (*7*), water-glycerol (10:1) mixture (*8*); egg lysozyme (□) at 0.04 (*1*), 0.35 (*2*), 0.60 (*3*), 0.80 (*4*), 0.96 (*5*); relative humidity degree, *R*, human serum albumin of the 0.04 ( r ) and 0.96 ( p ) relative humidity degree; α-chymotrypsin at 0.04 (□□), 0.65 (□■) and 0.96 (■■) relative humidity; radicals II and III in human serum albumin at 0.04 ( r , R ) and 0.96 ( p , L ) relative humidity [28,30].

suggest that the polarity and structure of the environment of the N-O group is the same in these matrices.

The deviation of the $g_{xx}$ — $A_{zz}$ correlation from that of model systems may be explained by the conformational changes in the radical structure caused by its protein environment.

The relaxation changes in the ESR spectra of spin-labeled samples were not observed at humidities less than 0.8 over the 130 — 320 K temperature range. This may be due to the rigid fixation of the radical fragment by nearby H-containing groups of the protein.

Heating the water-saturated sample results in considerable reversible broadening and a shift of major components of the ESR spectrum (Fig. 6b). In the 130 — 320 K temperature range a narrowing of the *x* component of the spectrum is observed due to averaging of the unresolved hyperfine structure (HFS) of radical and protein fragment protons. This observation suggests that there is a moistening effect on the molecular mobility in the sample even at low temperature (< 200 K). At temperatures higher than 250 K the *x* component of the ESR spectrum is shifted to low fields. This change cannot be explained by an increase in molecular mobility. Since there was no such effect in the lyophilized sample, it can be attributed to the weakening of the hydrogen bond between the N-O fragment and the water molecules in the vicinity.

Relaxation changes in the other components of the ESR spectrum of the water-saturated sample are observed above 260 K and can be explained by anisotropic rotational diffusion. It is probably caused by a weakening of the interaction between the radical N-O fragment and the surface protein groups and further hydration of the radical and protein groups. In this case, the water molecules appear to be speci-

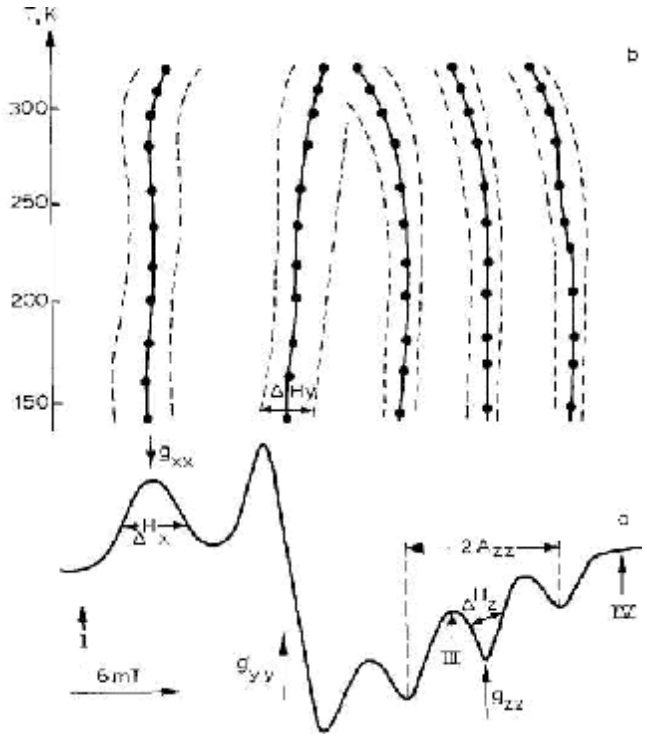


Fig. 6. The ESR spectra of radical I in egg lysozyme at 0.96 relative humidity recorded at 130 K at the 2-mm wave band (*b*) and the plot of the position ( , ------ , ) and half-width ( , - - - - , ) of the ESR spectrum components vs. temperature (*a*) [28]. I — IV: the position of the $Mn^{2+}$ standard components.

fic plasticizers of the protein globule mobility which in turn promotes radical rotation.

In the case of anisotropic motion broadening, the shifts of the principal values are different for canonic components of the ESR spectrum. In the ESR spectrum of spin-labeled lysozyme the *y* component is broader than the others because of weak anisotropy of the radical rotation round the z-axis. The theoretical calculation made by Antsiferova [28] has confirmed this supposition.

According to NMR data [29], the nitroxyl group of label **I** is 11 Å from the His-15 NH group and 10-11 Å from the Phe-3, Val-92 and Uso-88 protons. If the label is present in its extended conformation this would place the nitroxyl moiety near a cleft formed by the aforementioned hydrophobic groups. The rotational diffusion of the nitroxyl fragment in 2-mm ESR band remains slow, $\tau_c > 5 \cdot 10^{-8}$ s ($\tau_\perp > 1.1 \cdot 10^{-7}$ s, $\tau_\parallel > 2.2 \cdot 10^{-8}$ s), up to 305 K. Rotation is likely to occur round the -C-NH- and $-CH_2CO-$ bonds, whose direction is close to the *z*-axis of the radical *g*-tensor. The mobility is hindered by interaction with the protein and perhaps with the molecules of "viscous" water, close to the protein surface. The mobility depends on the microviscosity of the water-protein matrix in the label's vicinity. The effective local viscosity in the hydrophobic pocket of lysozyme is approx.

0.60 Pa s, as calculated according to the Stokes-Einstein equation at 300 K from 2-mm band spectra.

*Human serum albumin (HSA).* HSA samples labelled by radicals **I**—**III** have been studied [30]. Modification of the SH-groups of HSA by radicals **I** and **II** and the insertion of hydrophobic probe **III** were carried out as described [31]. The magnetic constants of HSA modified by these radicals (relative humidities 0.04 and 0.96) are presented in Fig. 5.

The magnetic constants of HSA modified by radicals **I** and **II** (humidity 0.04) fall close to the correlation $g_{xx}$ — $A_{zz}$ for model systems. This suggests that the structure and polarity of the microenvironment of these labels in lyophilized HSA sample is similar to that in frozen ethanol. An analysis of changes in the magnetic parameters of radicals **II** and **III** in model systems is required for the study of the influence of their structure and polarity on the microenvironment in HSA.

The ESR spectrum of HSA modified by label II contains a split *x* component due to the different types of interaction between radicals and environment in this system.

At higher humidities the radical fragment of label **I** is solvated by water molecules in a fashion similar to that in the water-glycerol mixture. Label **I** in HSA seems to be accessible to the aqueous environment. The same is true for other radicals bound to water-saturated HSA. However, various interactions of radicals **I** and II with the microenvironment may be proposed for water-saturated HSA.

*Liposome membranes.* The conformational and molecular dynamic properties of phospholipid bilayers are of extreme importance in understanding biochemical and biophysical processes in membranes.

A comparison of the molecular mobility of probes **IV** and **V** introduced into an aqueous suspension of phosphatidylcholine liposomes in phosphate buffer (pH 0.7; 0.02 M) with that of probe **VI** in an ethanol matrix has been made [32]. At 180 K the slope of the ESR spectra of the liposome membranes containing the probes differs only slightly from that in the frozen ethanol matrix. In the latter model system at temperatures < 160 K a splitting of the *x* component of the spectrum was observed which could be explained by the presence of several types of radical complexes with the solvent molecules.

Heating of the spin-labeled liposomal systems leads to the appearance of relaxation changes in the lineshape of their ESR spectra. The temperature-dependent changes in the width and the position of the ESR spectral components of the liposomal and model systems are illustrated in Fig. 7.

As seen from Fig. 7c, isotropic rotation of radical **VI** is observed in the ethanol matrix at temperatures above 150 K. However, in the liposomal system different changes are observed (Fig. 7a, b). In liposomes (besides the shift into the region of higher temperatures and weaker changes) there is a noticeably weaker broadening of the *x* and *z* components. These differences can be explained by the weak anisotropic rotation of the radical around the *y*-axis or by a decrease in the contribution to the line width of the unresolved HFS of the surrounding protons. The correlation time of probe rotation in the liposome membranes was $\tau_c \geq 10^{-7}$ s at 260 K within the Brownian diffusion model.

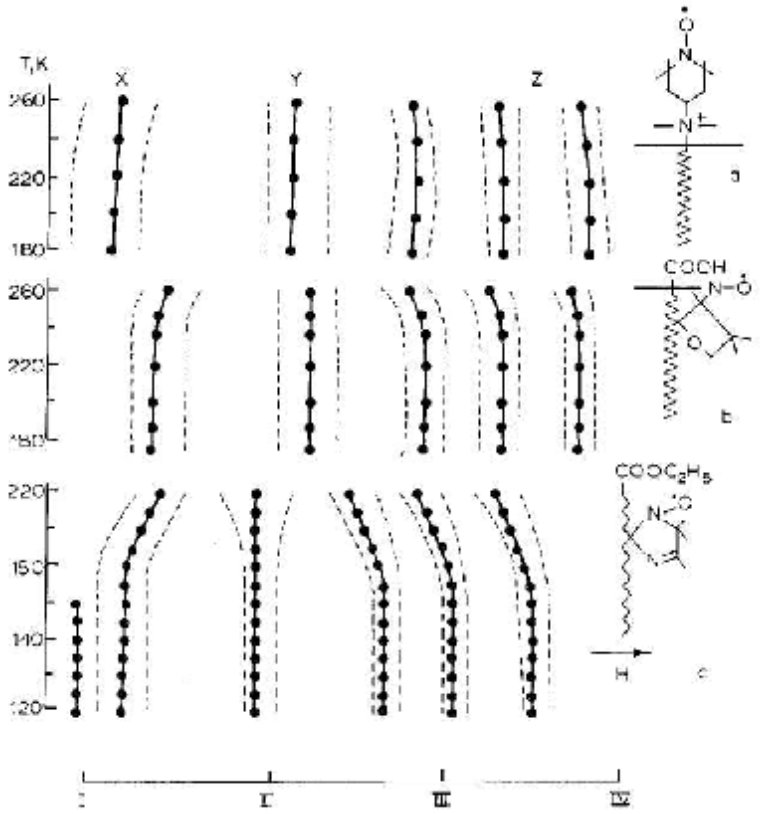


Fig. 7. The plot of the position ( , ----- , ) and half-width ( , - - - - , ) of the ESR spectra components of radicals **IV** (*a*), **V** (*b*) in liposome membranes and **VI** in ethanol (*c*) vs. temperature [32]. I-IV: position of the $Mn^{2+}$ standard components.

The relaxation changes in the ESR spectra of probe **IV** in membranes are observed at temperatures above 200 K. Similar changes in the ESR spectra of probe **V** reveal themselves at higher temperatures (≥ 240 K). However, they exhibit a sharper temperature-dependence. These differences can be explained by assuming that the positively charged nitroxyl fragment of probe **IV** is accessible to water located at the surface polar sites of the liposomal membrane [32], whereas the N-O fragment of probe **V** is in the lipid region [33].

The observed changes in line shape are complex, therefore more than one parameter, e.g., the correlation time, is needed for their description. However, a qualitative conclusion can be drawn, namely, that the frequency of probe mobility in the membranes at 260 K does not exceed $10^7$ $s^{-1}$, and the dependence of mobility on the temperature is mainly determined by the environment nearest to the probe. Thus, for probe **IV**, located in the surface layers of the membrane, the mobility increase at > 200 K is probably caused by the melting of the surface water matrix. Part of probe **V** is in a more rigid lipid part of the membrane adjacent to the surface layers. At higher temperatures the conformation of this region of the molecule changes and the increase in its mobility proceeds more sharply.

A comparison of the magnetic constants for the membranes modified by probe **V** with model systems containing similar radicals leads to the conclusion that the structure and polarity of the microenvironment are similar for probe **V** in membranes and probe **VII** in the frozen methanol matrix.

*Inverted micelles.* Solutions of surface active substances (SAS) in organic solvents are considered to be promising systems for various biochemical processes [34]. Due to their polar core, inverted micelles acquire the ability to solubilize ions, polar substances and a large number of water molecules. The catalytic activity of proteins trapped in the inner space of the micelles depends strongly on the polarity of the inner space and the structure of the micellar shell [35]. The properties of the micelle-protein system were studied by the method of spin labels and probes at the 3-cm wave band [6,35,36]. However, insufficient spectral resolution at this band did not allow the application of this method to the study of structural and dynamic parameters of this system.

The results are given below for the 2-mm wave band ESR investigation of the microenvironment polarity and dynamic properties of paramagnetic probe **VII** in the system shell of inverted micelles of sodium diisooctylsulfosuccinate in octane, containing solubilized protein α-chymotrypsin [37]. The samples were prepared according to the method of Belonogova et al. [35].

The magnetic constants of paramagnetic probe **VII** in frozen micellar systems with hydration degrees ($R$ = [$H_2O$]/[SAS]) from 0 to 80 and in some model systems are listed in the Appendix.

A comparison of the corresponding magnetic constants of micellar and model systems shows that probe **VII** in the micellar shell is present in a nonpolar environment and its magnetic parameters depend weakly on the hydration degree, $R$. Consequently, the radical fragment must be localized in the hydrophobic zone of the micellar shell and does not interact with the water molecules. Slight changes in the magnetic constants of the probe as a result of changes in system composition can be explained by the effect of the hydration degree on the size and general state of the micellar shell. The data obtained do not confirm the conclusion in [35], where the anomalously low $A_{zz}$ value of probe **VII** in the hydrated micelles was explained by its different localization in the matrix.

As the temperature increases above 200 K the components of the ESR spectra of the probe **VII** in micellar systems are broadened and shifted due to an increase in molecular mobility (Fig. 8). At 260 K the spectral components are combined into a wide (2 mT) singlet corresponding to radicals with the rotation frequency of $\nu_x \approx 10^8$ $s^{-1}$. Superimposed on this singlet is a triplet corresponding to radicals with a rotation frequency of $\nu_2 \approx 10^{10}$ $s^{-1}$ (see Fig. 8). A change in hydration degree from 3 to 80 leads to an increase in the g-factor of the second paramagnetic center. This shows that *4%* of the probe molecules extend beyond the lipid layer, where their mobility is high and they interact with water molecules solubilized in the inner space of the micelles. The difference between the g-factors of both paramagnetic centers can be explained by the different confirmation of the radical microenvironment in the shell and in the inner space of the micelles and by the dependence of the conformation of the radical microenvironment on the degree of hydration.

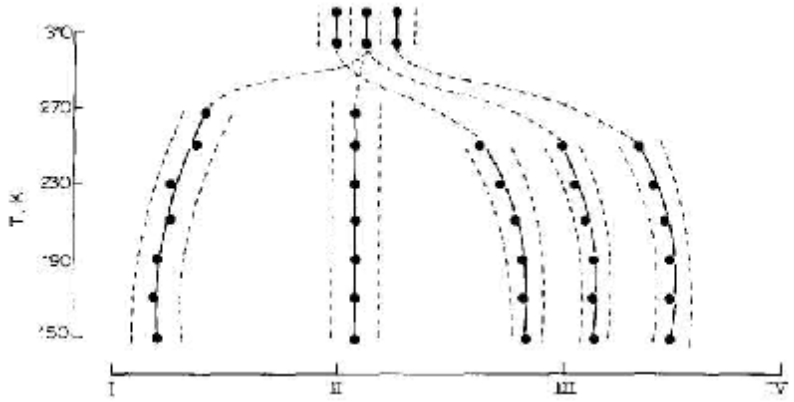


Fig. 8. The plot of the position ( , ----- , ) and half-width ( , - - - - , ) of the uniform ESR spectrum components of radical **VII** in inverted micelles vs. temperature [37]. I-IV: the position of the $Mn^{2+}$ standard components.

A comparison of the experimental ESR spectra with those tion to the eoretically calculated by Antsiferova and coworkers [37] showed that protein addition to the micellar system resulted in a 2-fold decrease in the activation energy of probe rotation. This provides evidence for a higher rigidity of the micellar structure at such a transition. The reverse effect is observed when the hydration degree of micelles is increased by protein.

The observed data can be explained by the cooperative effect of water and bioglobule on the micelle structure, since the microenvironment and mobility of the probe are remote from the interface.

α-*Chymotrypsin*. The catalytic activity of α-chymotrypsin depends on the structural organization and molecular mobility in the vicinity of its active center [38]. The introduction of a spin label into the zone of enzymatic reaction gives valuable information on the structural and dynamic parameters of this site which can be compared with the catalytic activity of α-chymotrypsin.

The results of the study of structural and dynamic characteristics of the environment of spin label **I** bound to methionine-192 group [39] in the region of the α-chymotrypsin active centers are presented in this section. A study of the enzyme at 0.04-0.96 humidity was carried out over the temperature range of 150-320 K.

The ESR spectra of lyophilised spin-labeled α-chymotrypsin at 150 K are characterized by less inhomogeneous broadening of the canonic components as compared with the egg lysozyme. This can be explained by the higher homogeneity of the label environment in α-chymotrypsin. Nevertheless a considerable broadening of the spectral components of the 0.96-humidity sample (Fig. 9) is observed, which can be caused by conformational changes in the sample during its wetting.

The magnetic parameters $g_{xx}$ and $A_{zz}$ of radical I located in the vicinity of the active center of frozen α-chymotrypsin at relative humidities of 0.04, 0.65 and 0.96 are presented in Fig. 5. As seen from the figure, the magnetic parameters of the lyophilized sample practically coincide with the general $g_{xx}$ — $A_{zz}$ correlation of model systems. This demonstrates the similarity of the polarity and structure of

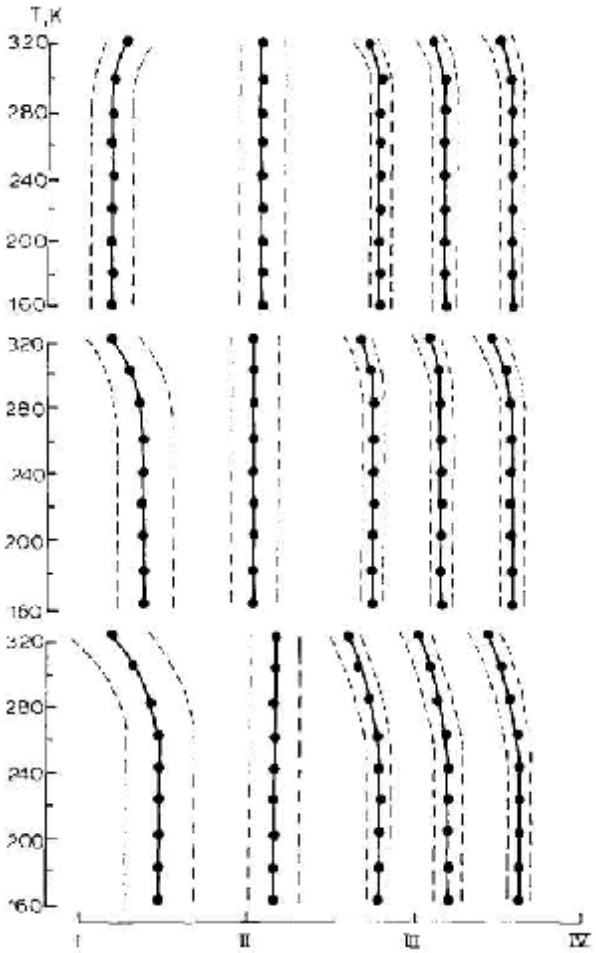


Fig. 9. The plot of the position ( , ----- , ) and half-width ( , - - - , ) of the ESR spectra components of radical **I** in α-chymotrypsin with the 0.04 (*a*), 0.65 (*b*) and 0.96 (*c*) value of relative humidity degree vs. temperature. I — IV: position of the $Mn^{2+}$ standard components.

radical **I** environment in the lyophilized sample and ethanol matrix. As the sample is saturated by water the active fragment of label **I** (as in the case of HSA) becomes solvated with its molecules forming an *n*-σ radical complex as evidenced by the gradual changes in its magnetic parameters. The polarity of the radical microenvironment increases by 1.4 and 1.8 times as the relative humidity increases from 0.04 to 0.65 and 0.96, respectively. Different slopes of the $g_{xx}$ — $A_{zz}$ correlation plots of radical **I** in model systems and α-chymotrypsin probably indicate the predominance of the donor-acceptor radical complex over an electrostatic complex in this biological system.

The ESR spectra of the lyophilized spin-labelled α-chymotrypsin did not exhibit any relaxation changes in the line shape up to 290 K which is explained by the rigid fixation of the radical fragment by the surrounding groups. At higher temperatures label mobility increases (see Fig. 9a). The correlation times of the label rotation

defined from the ESR spectra were equal to $\tau_c = 6 \cdot 10^{-19} \exp(-8.0 \cdot 10^4/RT)$ and the effective microviscosity of the radical environment at 300 K was 72 Pa s.

As the sample becomes hydrated molecular mobility is registered at lower temperatures (Fig. 9b, c). The analysis of the experimental data showed that in α-chymotrypsin the rotation of radical I proceeds around the *y* axis with correlation times of $\tau_c = 3.6 \cdot 10^{-12} \exp(-2.6 \cdot 10^4/RT)$ and $\tau_C = 4.1 \cdot 10^{-11} \exp(-1.8 \cdot 10^4/RT)$ at sample humidities of 0.65 and 0.96, respectively. The value of the effective viscosity at the radical location decreased from 72 to 15 and 7 Pa s as the relative humidity increased from 0.04 to 0.65 and 0.96. In contrast to the lyophilized sample, the *x* component of the ESR spectra of hydrated a-chymotrypsin samples shifts to lower fields upon heating (Fig. 9b, c). This effect and the same effect in other spin-labelled biological systems may be explained by the weakening of the hydrogen bond of the radical complex in the hydrated α-chymotrypsin as the temperature increases.

Thus, the molecular motion of label **I** in lyophilyzed α-chymotrypsin is hindered by strong interaction of its nitroxyl fragment with hydroxyl groups. In the radical complex the latter are partially substituted by water molecules during sample hydration, which leads to an increase in the radical dynamics. Since the motion of the label was completely frozen in egg lysozyme at relative humidities up to 0.8, the conclusion can be made that the radical in α-chymotrypsin has some odd degrees of freedom as compared with lysozyme and is located in a hydrophobic pocket of different structure. This is confirmed by the difference in radical axis of the predominant rotation and the character of its interaction with the environment in these systems. The correlation time of radical rotation in α-chymotrypsin decreases to $5.5 \cdot 10^{-11}$ s in the above mentioned micellar systems with the hydration degree, $N = 6$ [35].

*Cotton fibre and cellulose.* To determine the mechanisms of chemical conversions in cotton fiber and cellulose it is necessary to know their microstructure and dynamic properties. ESR spectroscopy has been widely applied to the solution of this problem [40,41]. However, in the case of these natural biopolymers, as well as in the above discussed ones, low spectral resolution of the conventional 3-cm ESR wave band does not give the complete picture of the processes in these systems. High spectral resolution ESR was used in the study of structural and dynamic parameters of the modified cotton fiber [42] and microcrystalline cellulose [43].

Cotton fiber from the 5595-V and Tashkent-1 cotton strains and microcrystalline cellulose (C) amorphised under 20 kbar pressure between Bridgeman anvils with 10° and 400° shift (CA-I and CA-II, respectively) were investigated. Spin labelling fiber and cellulose by radical **VIII** was carried out according to previously described procedures [44]. The C and CA-I samples were exposed to $^{60}$Co radiation (10 Mrad, 290 K) in air.

At 150 K the ESR spectra of lyophilized spin-labeled systems, like those of egg lysozyme, were characterized by considerable broadening of the canonic lines caused by the interaction of the nitroxyl fragment with hydroxyl groups of proteins. The magnetic constants of radical **VIII** in the biological and model systems estimated from their ESR spectra are given in the Appendix.

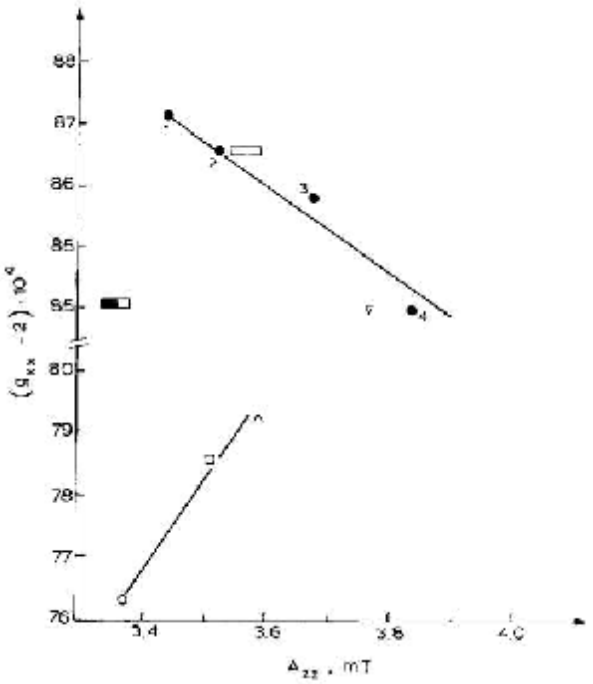


Fig. 10. The correlation plot $g_{xx}$ — $A_{zz}$ for radical **VIII** in frozen (150 K) octane (*1*), ethanol (*2*), methanol (*3*), water-glycerol (10:1) mixture (*4*) and in cotton fibres "Tashkent-1" (□□), "Tashkent-1" infected by vylt (□■), 5595-V (D), cellulose samples C ( , ), CA-I ( 8 ) and Ca-II (□) with the 0.04 value of relative humidity degree [42,43].

Values of the magnetic constants $g_{xx}$ and $A_{zz}$ of radical **VIII** are summarized in Fig. 10. This figure shows that the magnetic parameters of 5595-V and Tashkent-1 samples fall into the $g_{xx}$ — $A_{zz}$ correlation for the model systems. This observation leads to the conclusion that the structure and polarity of the microenvironment of radical **VIII** are identical in the Tashkent-1 sample and ethanol matrix as well as in the 5595-V sample and water matrix.

Quite a different picture is observed for the spin-labelled sample of cellulose and cotton fibre from Vylt-infected Tashkent-1. Their magnetic constants fall out of the general $g_{xx}$ — $A_{zz}$ correlation of frozen model systems (see Fig. 10). This can be explained by conformational difference in the label **VIII** microenvironment in these biological polymers.

On heating of the 5595-V and C samples the *x* components of their ESR spectra gradually shifted towards low field (Fig. lla,b, respectively). As in the case of lysozyme, this is likely to be caused by the weakening of the hydrogen bond between the radical fragment and molecules of the microenvironment at elevated temperatures.

At 315 K the *y* component of the ESR spectrum of the lyophilized sample of 5595-V is a superposition of at least two lines, i.e., a wide singlet and a triplet with $g$ = 2.00610 and $a$ = 1.52 mT (Fig. 11a). The triplet is due to the presence of amorphous regions of high radical mobility ($\tau_c < 2.2 \cdot 10^{-10}$ s, 335 K). An estimation

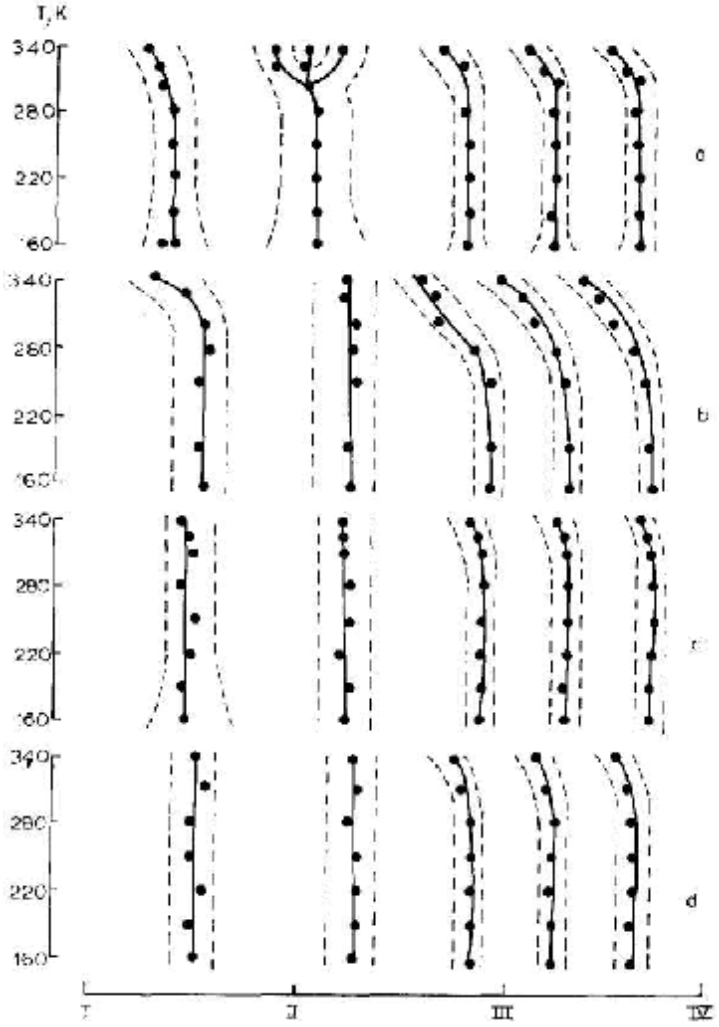


Fig. 11. The plot of the position ( , -------- , ) and half-width ( , - - - - - , ) of the ESR spectra components of radical VIII in lyophilized cotton fibres 5595-V (*a*), cellulose samples C (*b*), CA-I (*c*) and CA-II (*d*) vs. temperature [42,43]. I — IV: position of the $Mn^{2+}$ standard components.

of the radical portion in the amorphous phase (about 2%) agrees with the value obtained earlier at the 3-cm wave band [40]. The difference in the spin label isotropic g-factors in the crystalline (2.00553) and amorphous (2.00610) phases agrees with the shift of the *x* component to lower field as the temperature increases and shows that the intensification of the molecular motion in the amorphous regions of the 5595-V sample is accompanied by a weakening hydrogen bonds formed between the radical and its microenvironment.

Different phases in cellulose were not detected.

The heating of the spin-labeled 5595-V samples results in the shift (0.7 mT) and the broadening (0.08 mT) of the *z* component (Fig. lla). Such a weak broadening of the line accompanied by a considerable shift is at variance with the model of

Brownian isotropic rotation and with the model of large angle jumps [40,45]. This effect can be explained either by compensative narrowing of the line due to the decrease in inhomogeneous broadening or by the presence of fast torsion oscillations of the radical fragment [46] with a frequency of $10^9$ $s^{-1}$ and amplitude of $10 \pm 3°$ (335 K) near the *x*-axis.

Analysis of the temperature dependence of broadening and the shift of the *z* component of the ESR spectra of the spin-labeled cellulose samples (Fig. llb-d) as well as a comparison with the corresponding changes in theoretically calculated ESR spectra [47] leads to the conclusion that label **VIII** undergoes Brownian rotation about the axis of preferred rotation in the *xz* plane of the molecular coordinate system.

The amorphization of sample C leads to a decrease in the mobility of the label CA-I and to partial reduction of the elasticity of the label environment (see Fig. lib). The correlation time, $\tau_c$, of the radical **VIII** rotation in C, CA-1 and CA-II samples calculated from the ESR spectra are equal to $2.3 \cdot 10^{-4} \exp(-1.9 \cdot 10^4/RT)$, $36 \exp(-4.6 \cdot 10^4/RT)$ and $5.0 \cdot 10^{-2} \exp(-3.1 \cdot 10^4/RT)$ s, respectively.

Thus, radical mobility is mainly determined by the shape of the cage which the radical occupies in cellulose and the degree of its treatment which is likely to decrease the space size and to affect the system conformation. The treatment effect probably reflects a change in the conformation of the macromolecule and its monomeric subunits.

To confirm the latter supposition the ESR spectra of γ-radiated C (*a*, *b*) and CA-II (*c*, *d*) samples were recorded at the 3-cm (*a*, *c*) and 2-mm (*b*, *d*) wave bands at 290 K (see Fig. 12).

A comparison of the ESR spectra leads to the conclusion that in sample C there are at least three paramagnetic centers of differing magnetic constants (see Fig. 12): $R_1$ is a singlet ($g_1 = 2.00281$), $R_2$ is a doublet ($g_2 = 2.00295$ and $a_2 = 2.9$ mT) and $R_3$ is a triplet ($g_3 = 2.00442$ and $a_3 = 2.7$ mT). This observation mainly agrees with the

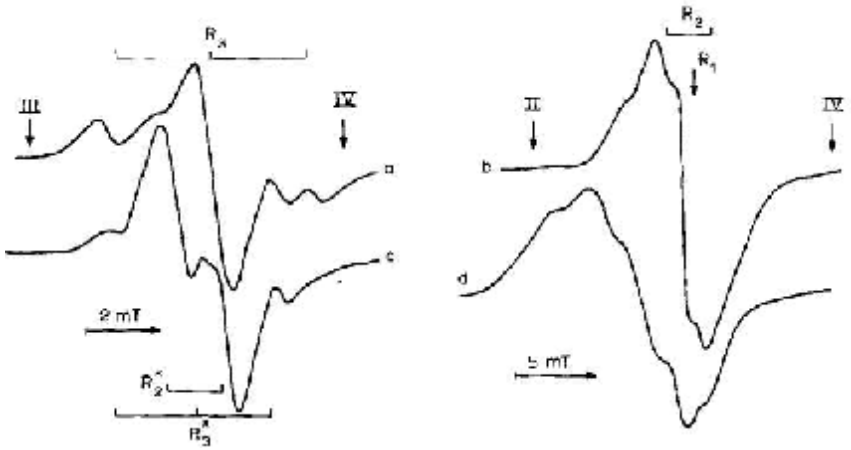


Fig. 12. The ESR spectra of γ-radiated (10 Mrad) samples of lyophilized cellulose C (*a*, *b*) and Ca-II (*c*, *d*) registered at 290 K in 3-cm (*a*, *c*) and 2-mm (*b*, *d*) wave bands [43]. II-IV: position of the $Mn^{2+}$ standard components.

results of the mathematic modeling of the 3-cm ESR spectra of the γ-irradiated C sample [41]. The $R_1$ line can be attributed to contamination of lignin [41]. The formation of $R_2$ and $R_3$ centers can be explained by the process of dehydrogenation of the glucopyranose cycle in the $C_1$ and $C_4$ positions, respectively.

In CA-1I after radiation at least two additional paramagnetic centers appear (see Fig. 12): $R_2^*$ is a doublet ($g_2^*$ = 2.00505 and $a_2^*$ = 1.5 mT) and $R_3^*$ is a triplet ($g_3^*$ = 2.00532 and $a_3^*$ = 2.2 mT). Since the C-monomer unit can exist in different conformations, the formation of these centers in CA-II can be explained by dehydrogenation of a glucopyranose ring (conformation of which is different from the initial one) in the $C_1$ and $C_4$ positions, respectively.

*A nisotropic slow molecular rotations studied by the method of RF saturation transfer at the 2-mm wave band ESR*

As known, the "linear" ESR method is used to study molecular processes in biological and other systems with correlation times of $\tau_c = 10^{-11}$ — $10^{-7}$ s. However, slow transformations with a characteristic time of $\tau_c \geq 10^{-7}$ s occur in major biological native systems. These processes can be studied with the help of RF saturation transfer ESR (ST ESR) [5,48].

According to the ST ESR approach, the shape of the ESR spectrum of the spin-labeled system recorded under the conditions of saturation,

$$\gamma^2 H_1^2 T_1 T_2 >> 1 \qquad (6)$$

and adiabatic fast passage of a resonance,

$$dH/dt = \gamma H_m \omega_m >> \gamma^2 H_1^2 \qquad (7)$$

(where γ is the gyromagnetic ratio, $H_1$ is the magnetic component of the MW field in the sample, $T_1$ and $T_2$ are the spin-lattice and spin-spin relaxation times, respectively, $dH/dt$ is the rate of the magnetic field change, and $H_m$ and $\omega_m$ are the amplitude and angle frequency of the a.c. modulation field, respectively), is sensitive both to their effective relaxation time and to slow ($10^{-7} \leq \tau_c \leq 10^{-3}$ s) molecular motions. In phase and π/2 out of phase components of the dispersion and absorption signals are more sensitive to such coincident relaxation and dynamic processes [5,24].

As a rule, motion in biological systems is anisotropic. Consequently the relationships shown in Eqns. 6 and 7 may not be satisfied when a radical rotates slowly around, for example, a preferred *x*-axis for radicals whose orientation in the magnetic field was determined by their motion about the *y*- and z-axes. In this case spectral diffusion of RF saturation occurs and the amplitudes of the *y* and z spectral components decrease. Theoretical analysis shows that at low RF frequency, the determination of the preferable radical rotating axis and the separation of the radical relaxation and motions are impossible because the ST ESR principal components overlap [5].

These limitations are partly eliminated when ESR spectra are recorded at higher frequency. However, the anisotropy of the *g*-factor and HFI at frequencies up to 30

GHz are comparable [49], so that some overlapping of the SR ESR spectral components remains.

Previously [50,51] we have shown that the above-mentioned limitations of the ST ESR method may be eliminated completely by recording ESR spectra at the 2-mm wave band. According to theory, both the rate of MW saturation transfer in the spectrum and the spectrum shape's sensitivity to low anisotropic molecular moving should increase.

The ESR and ST ESR spectra of radicals **IX** and **X** dissolved in *tert*-butylbenzene ($10^{-2}$ M) were recorded at 90-300 K and $H_1$ = 20 μT. These radicals are characterized by highly anisotropic rotation in the model systems around the *x*- and *y*-axes, respectively. The magnetic constants of radicals **IX** and **X** are listed in the Appendix.

At temperatures ≥ 180 K the motion of the radicals is anisotropic with a correlation time of $\tau_c \leq 10^{-7}$ s. Extrapolation to 160 K gave a value of $\tau_c = 5 \cdot 10^{-7}$ s. At < 170 K the shape of the first harmonic of the in phase absorption does not change appreciably. Marked changes in the bell-like ST ESR spectra are observed in the range 130-170 K.

Theoretical calculations made by Livshits [51] showed that the ratio of the amplitude of the second harmonic of π/2 out of phase to the in-phase component of the absorption signal is sensitive only to the time of spin-lattice relaxation, $T_1$. The ratio of the amplitudes of the components of its π/2 out-of-phase ST ESR spectrum is sensitive to the radical rotation.

For example, the amplitude ratio of the *x* and *y* components of the π/2 out-of-phase ST ESR spectra of radical IX increases from 0.4 to 0.75 at 130-170 K (Fig. 13a). This provides evidence for an increase in the rotation rate of **IX** about the

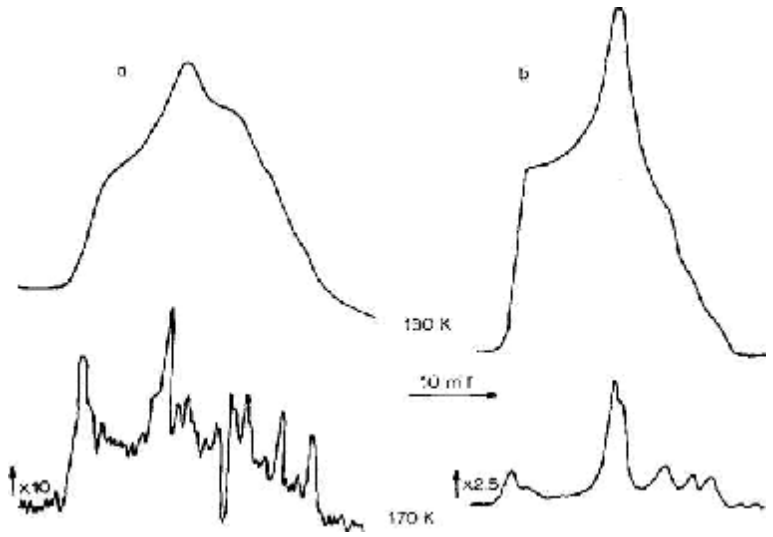


Fig. 13. The second harmonic π/2-out-of-phase of absorption signals of radical **IX** (*a*) and **X** (*b*) solutions in *tert*-butylbenzene at 130 and 170 K [50,51].

*x*-axis with a correlation time of $\tau_c \geq 4 \cdot 10^{-6}$ s, whereas the value of the spin-lattice relaxation time $T_1$ changes by a factor of 6-10.

More considerable changes are observed for radical **X** (Fig. 13b). The same temperature increase leads to a decrease in the rotational correlation time of this radical by more than two orders of magnitude ($10^{-5}$-$10^{-7}$ s) accompanied by only a very slight (1.5-2 times) decrease in the $T_1$ value.

Thus, the changes in the ST ESR spectra of radical **IX** are caused by a decrease both in the value of spin-lattice relaxation time $T_1$, and in radical rotation around the *x*-axis, while those of radical **X** are caused mainly by intensification of very slow rotation around its long axis. If spin-lattice relaxation is mainly determined by very fast radical motions limited in their amplitude, rotational mobility is characterized by slower ($\tau_C \approx (10^{-5}$-$10^{-7}$ s) motion with relatively large angular amplitude. The differences in the dynamics of radicals **IX** and **X** perhaps can be explained by their structural differences and the peculiarities of interaction with the environment.

Consequently, the 2-mm ST ESR registration essentially expands the potentialities of the method in the investigation of anisotropic, very-slow-molecular mobility in various biological systems.

*Identification of the paramagnetic centers via the 2-mm hand ESR spectra*

ESR spectroscopy is widely used to study metabolic and radiation-induced reactions in biological systems, in which paramagnetic centers are formed both as transients and as final products [52]. An analysis of the nature and character of these centers makes it possible to study the reactions and structural, conformational and dynamic properties of radical microenvironment in biological systems.

Paramagnetic centers with unpaired electrons localized on carbon or sulfur atoms are as a rule primary radicals in biological systems. In the former case, the *g*-factor of the paramagnetic center is usually close to that of the free electron ($g_e$ = 2.00232). HFI of the unpaired electron with the other nuclei with nonzero nuclear spin is easily analyzed according to the ESR spectra at the wide range of detection frequency [52-54]. The localization of the unpaired electron on the sulfur atom causes a substantial deviation of the *g*-factor from the $g_e$ and leads to its tensor character. Magnetic parameters of such a center may be determined from their ESR spectra recorded at the 3-cm wave band [55].

Peroxide radicals (PR) are rather formed as both intermediate and final products in biological systems. The unpaired electron in such centers localizes mainly on the O-O fragment; therefore HFS is absent, the values of their *g*-factors are close to each other [55], and the identification of PR in the 3-cm ESR spectra is difficult.

As in the case of nitroxide radicals detected at the 2-mm wave band of ESR all the components of the PR's ESR spectra are resolved [56]. Simultaneous observation of paramagnetic centers which are different in their nature but close in their *g*-factors is possible at this band. In [57] the possibility of identifying organic PR via their paramagnetic constants (see Appendix) was analyzed.

In the case of PR the main contribution to the *g*-factor is made by the $n\pi^*$ excited electron configuration [58]. Therefore, a comparison of experimental and

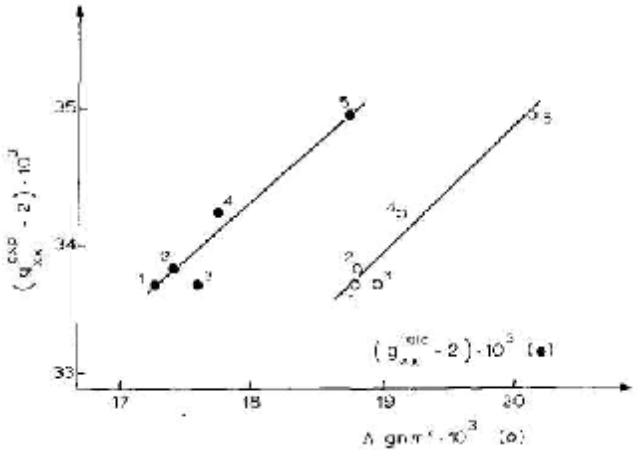

Fig. 14. The correlation plots $g_{xx}^{exp} - g_{xx}^{calc}$ and $g_{xx}^{exp} - \Delta g_{n\pi^*}^{calc}$ of peroxy radicals $C_3H_7CH_2OO^{\bullet}$ (*1*), $C_3H_7(CH_3)_2COO^{\bullet}$ (*2*), $(CH_3)_3COO^{\bullet}$ (*3*), $C_2H_5(CH_3)_2COO^{\bullet}$ (*4*), and $C_2H_5CH_2OO^{\bullet}$ (*5*) [57].

theoretical magnetic parameters of some PR, calculated by the method of Dmitruk [57], was undertaken to determine the possibility of PR identification.

The correlation of experimental and theoretical magnetic parameters of some primary and tertiary PR is shown in Fig. 14. The $\Delta g_{n\pi^*}^{calc}$-shift of the $g$-factor is caused by the $n\pi^*$ transition. For secondary PR the calculation gives anomalously low values of magnetic constants [57].

As seen from Fig. 14, the magnetic parameters of organic PR are strongly dependent on the donor-acceptor and conformational properties of their substituents. This makes possible the identification of primary and tertiary PR formed in biological systems.

Thus, high resolution ESR spectroscopy permits the identification of paramagnetic centers with different properties and close g-factors, and the use of stable [e.g., $(C_6H_5)_3COO^{\bullet}$] PR as spin labels in the study of biological macromolecules.

## Conclusion

The data presented in this review show that 2-mm wave band ESR makes it possible to obtain qualitatively new information in such fields as metrology of free radicals, spin labels and probes, molecular mobility, electron and spatial structures of paramagnetic centers, local effects of the matrix, etc. Separate registration of the ESR spectra of paramagnetic centers of different natures makes possible the analysis of structural and dynamic characteristics of spin-labeled biological objects.

Thus, the ESR spectroscopy of high resolution combined with the method of spin labels and probes gives a unique possibility of analyzing fine structure and dynamic transitions in various biological systems. The above results show high resolution ESR spectroscopy to be an efficient method for the solution of a wide range of problems in chemical and biological physics.

The further development of the method is its combination with pulsed methods and Fourier data processing of spectra of biological paramagnetic centers at the 2-mm wave band of ESR spectroscopy.

**Acknowledgements**

The author expresses his sincere gratitude to Prof. G.I. Likhtenstein and Dr A.V. Kulikov for their sustained attention to this work and valuable criticism, and to Prof. Ya.S. Lebedev and Dr O.Ya. Grinberg for their participation in the discussion of the results.

## Appendix

I. Magnetic constants of nitroxyl radicals in frozen biological and model systems [17].

| Matrix | $R$ | $g_{zz}$ | $g_{yy}$ | $g_{zz}$ | $g_{iso}$ | $A_{zz}$ (mT) |
|---|---|---|---|---|---|---|
| | | | Radical **I** | | | |
| Toluene | – | 2.00953 | 2.00577 | 2.00176 | 2.0569 | 3.40 |
| *n*-Butanol | – | 2.01010 | | | | |
| | | 2.00935 | 2.00602 | 2.00197 | 2.00578 | 3.50 |
| Ethanol | – | 2.00910 | 2.00573 | 2.00210 | 2.00564 | 3.58 |
| Ethanol + water | 0.25 | 2.00902 | 2.00543 | 2.00212 | 2.00552 | 3.60 |
| Ethanol + water | 0.50 | 2.00890 | 2.00602 | 2.00214 | 2.00569 | 3.65 |
| Ethanol + water | 0.66 | 2.00883 | 2.00608 | 2.00201 | 2.00564 | 3.70 |
| Methanol | | 2.00860 | 2.00550 | 2.00178 | 2.00529 | 3.73 |
| Water + glycerol | 0.90 | 2.00834 | 2.00571 | 2.00167 | 2.00524 | 3.77 |
| HSA | 0.04 | 2.00893 | 2.00585 | 2.00164 | 2.00547 | 3.60 |
| HSA | 0.96 | 2.00842 | 2.00570 | 2.00170 | 2.00527 | 3.75 |
| Lysozyme | 0.04 | 2.00946 | 2.00646 | 2.00217 | 2.00603 | 3.50 |
| Lysozyme | 0.35 | 2.00923 | 2.00617 | 2.00220 | 2.00587 | 3.61 |
| Lysozyme | 0.60 | 2.00912 | 2.00614 | 2.00214 | 2.00580 | 3.69 |
| Lysozyme | 0.80 | 2.00908 | 2.00603 | 2.00211 | 2.00574 | 3.74 |
| Lysozyme | 0.96 | 2.00902 | 2.00624 | 2.00211 | 2.00579 | 3.85 |
| α-Chymotrypsin | 0.04 | 2.00912 | 2.00598 | 2.00210 | 2.00573 | 3.58 |
| α-Chymotrypsin | 0.65 | 2.00859 | 2.00613 | 2.00219 | 2.00564 | 3.67 |
| α-Chymotrypsin | 0.96 | 2.00828 | 2.00583 | 2.00209 | 2.00540 | 3.73 |
| | | | Radical **II** | | | |
| HSA | 0.04 | 2.00998 | | | | |
| | | 2.00883 | 2.00612 | 2.00216 | 2.00570 | 3.64 |
| HSA | 0.96 | 2.00863 | 2.00613 | 2.00215 | 2.00563 | 3.84 |
| | | | Radical **III** | | | |
| HSA | 0.04 | 2.00855 | 2.00621 | 2.00214 | 2.00563 | 3.55 |
| HSA | 0.96 | 2.00845 | 2.00614 | 2.00210 | 2.00556 | 3.67 |
| | | | Radical **IV** | | | |
| Membranes | – | 2.00980 | 2.00642 | 2.00232 | 2.00618 | 3.67 |
| | | | Radical **V** | | | |
| Membranes | – | 2.00918 | 2.00614 | 2.00230 | 2.00587 | 3.60 |
| | | | Radical **VI** | | | |
| Ethanol | – | 2.01044 | | | | |
| | | 2.00984 | 2.00696 | 2.00302 | 2.00661 | 3.39 |
| | | | Radical **VII** | | | |
| Octane | – | 2.00951 | 2.00611 | 2.00215 | 2.00592 | 3.28 |
| *n*-Propanol | – | 2.00955 | | | | |
| | | 2.00894 | 2.00619 | 2.00217 | 2.00597 | 3.29 |
| Ethanol | – | 2.00901 | 2.00617 | 2.00219 | 2.00597 | 3.42 |
| Methanol | – | 2.00882 | 2.00626 | 2.00228 | 2.00579 | 3.61 |
| Micelles without | | | | | | |
| the protein | 0 | 2.00952 | 2.00626 | 2.00226 | 2.00601 | 3.41 |
| | 3 | 2.00946 | 2.00614 | 2.00213 | 2.00591 | 3.32 |
| Micelles with | | | | | | |
| the protein | 3 | 2.00954 | 2.00622 | 2.00221 | 2.00599 | 3.34 |
| | 6 | 2.00958 | 2.00622 | 2.00231 | 2.00603 | 3.41 |

## Appendix (continued)

I. Magnetic constants of nitroxyl radicals in frozen-biological and model systems [17].

| Matrix | *R* | $g_{zz}$ | $g_{yy}$ | $g_{zz}$ | $g_{iso}$ | $A_{zz}$ (mT) |
|---|---|---|---|---|---|---|
| α-Chymotrypsin | 10 | 2.00950 | 2.00618 | 2.00215 | 2.00594 | 3.36 |
| | 15 | 2.00954 | 2.00622 | 2.00220 | 2.00599 | 3.41 |
| | 20 | 2.00950 | 2.00622 | 2.00230 | 2.00601 | 3.36 |
| | 30 | 2.00946 | 2.00621 | 2.00222 | 2.00597 | 3.41 |
| | 40 | 2.00939 | 2.00618 | 2.00217 | 2.00591 | 3.32 |
| | 50 | 2.00943 | 2.00614 | 2.00217 | 2.00591 | 3.32 |
| | 60 | 2.00946 | 2.00622 | 2.00226 | 2.00598 | 3.35 |
| | 80 | 2.00937 | 2.00607 | 2.00210 | 2.00585 | 3.34 |
| | | | Radical **VIII** | | | |
| Octane | – | 2.00872 | 2.00633 | 2.00214 | 2.00573 | 3.43 |
| Ethanol | – | 2.00865 | 2.00622 | 2.00221 | 2.00569 | 3.52 |
| Methanol | – | 2.00857 | 2.00617 | 2.00209 | 2.00560 | 3.69 |
| Water + glycerol | 0.90 | 2.00840 | 2.00627 | 2.00215 | 2.00561 | 3.81 |
| Cotton 5595-V | 0.04 | 2.00842 | 2.00592 | 2.00224 | 2.00553 | 3.76 |
| Cotton "Tash-1" | 0.04 | 2.00863 | 2.00622 | 2.00232 | 2.00572 | 3.55 |
| Cotton "Tash-1" + vylt | 0.04 | 2.00840 | 2.00562 | 2.00212 | 2.00538 | 3.35 |
| C | 0.04 | 2.00762 | 2.00582 | 2.00211 | 2.00518 | 3.37 |
| CA-I | 0.04 | 2.00791 | 2.00584 | 2.00222 | 2.00532 | 3.57 |
| CA-II | 0.04 | 2.00783 | 2.00574 | 2.00227 | 2.00528 | 3.49 |
| | | | Radical **IX** | | | |
| *t*-Butylbenzene | – | 2.00979 | 2.00622 | 2.00206 | 2.00602 | 3.41 |
| | | | Radical **X** | | | |
| *t*-Butylbenzene | – | 2.00947 | 2.00541 | 2.00217 | 2.00568 | 3.12 |

N.B.: The measurement errors in the component of *g*- and *A*-tensors are $7 \cdot 10^{-5}$ and $3 \cdot 10^{-2}$ mT, respectively. *R* is the relative $H_2O$ content (in model systems), hydration degree (in micelles) and the value of relative humidity (in other biosystems).

## Appendix (continued)

II. Magnetic constants of organic peroxyradicals in model systems [56]

| Radical | Matrix | $g_{zz}$ | $g_{yy}$ | $g_{zz}$ | $g_{iso}$ |
|---|---|---|---|---|---|
| $HOO^{\bullet}$ | $H_2O_2 + H_2O$ | 2.0329 | 2.00806 | 2.00331 | 2.01478 |
| $(CF,(CF_2)_X)_2CFOO^{\bullet}$ | self | 2.0381 | 2.00742 | 2.00231 | 2.01596 |
| $CF_3(CF_2)_XCF_2OO^{\bullet}$ | self | 2.0396 | 2.00770 | 2.00277 | 2.01670 |
| $C_6H_HOO^{\bullet}$ | self | 2.0340 | | | |
| | | 2.0306 | 2.00815 | 2.00279 | 2.01498 |
| $(C_6H_5)_3COO^{\bullet}$ | $(C_6H_5)_3CC1$ | 2.0310 | 2.01445 | 2.00200 | 2.01581 |
| $(C_6H_5)_2CHOO^{\bullet}$ | self | 2.0346 | 2.00792 | 2.00212 | 2.01488 |
| $Br(QH_4)C(CH_3)_2OO^{\bullet}$ | self | 2.0328 | | | |
| | | 2.0228 | 2.00792 | 2.00236 | 2.01436 |
| $(C_6H_5)C(CH_3)_3OO^{\bullet}$ | self | 2.0334 | | | |
| | | 2.0302 | 2.00824 | 2.00253 | 2.01472 |
| $(CH_3)_3COO^{\bullet}$ | self | 2.0336 | 2.00830 | 2.00237 | 2.01476 |
| $C_2H_5(CH_3)_2COO^{\bullet}$ | self | 2.0342 | 2.00859 | 2.00267 | 2.01415 |
| $C_3H_7(CH_3)_2COO^{\bullet}$ | self | 2.0337 | 2.00801 | 2.00251 | 2.01474 |
| $C_3H_7(CH_3)HCOO^{\bullet}$ | self | 2.0340 | | | |
| | | 2.0295 | 2.00823 | 2.00240 | 2.01487 |
| $C_3H_7CH_2OO^{\bullet}$ | self | 2.0336 | 2.00816 | 2.00358 | 2.01511 |
| $C_2H_3CH_2OO^{\bullet}$ | $^{t}$Bu-butyrate | 2.0349 | 2.00792 | 2.00271 | 2.01518 |
| $CH_3CONHCHC_3H_7$ $OO^{\bullet}$ | self | 2.0323 | 2.00802 | 2.00187 | 2.01418 |
| $CH_3CON(CH_3)CH_2OO$ | self | 2.0350 | 2.00792 | 2.00180 | 2.01490 |
| $CH_3CON(C_2H_5)C_2H_4OO$ | self | 2.0351 | | | |
| | | 2.0309 | 2.00780 | 2.00181 | 2.01489 |
| $CH_3CONHCHCH_3$ $OO^{\bullet}$ | self | 2.0320 | 2.00766 | 2.00339 | 2.01435 |

N.B.: The measurement errors of the $g_{xx}$ and $g_{yy}$, $g_M$ values are $2 \cdot 10^{-4}$ and $3 \cdot 10^{-5}$, respectively. The magnetic constants of alkyl radicals formed in some systems are not listed. Peroxyradicals were produced mainly by photolysis of respective hydroperoxide at 77 K.

## References


1 Konev, S.V. (1965) Electron Excited States of Biopolymer (Russ), Nauka i Technika, Minsk.
2 Goldansky, V.I. (1963) Mossbauer Effect and Its Application to Chemistry (Russ), USSR Acad. Nauk Publ., Moskou.
3 Kiselyov, N.A. (1965) Electron Microscopy of Biological Molecules (Russ). Nauka, Moskou.
4 Berliner, L. (Ed.) (1976) Spin Labeling. Theory and Application. Vol. 1, Academic Press, New York.
5 Berliner, L. (Ed.) (1979) Spin Labeling. Theory and Application. Vol. 2, Academic Press, New York.
6 Likhtenstein, G.I. (1974) Spin Labels in Molecular Biology (Russ). Nauka, Moskou.
7 Likhtenstein, G.I. (1988) Chemical Physics of Metalloenzyme Catalysis. Springer Verlag, Heidelberg.
8 Dudich, I.V., Timofeev, V.P., Volkenstein, M.V. and Misharin, A. Ju. (1977) Mol. Biol. 11, 685-689.
9 Isaev-Ivanov, V.V., Lavrov, V.V. and Fomichev, V.N. (1976) Dokl. Akad. Nauk USSR 229, 70-72.
10 Hyde, J.S. and Dalton, L. (1972) Chem. Phys. Lett. 16, 568-572.
11 Hwang, J.S., Mason, R., Hwang, L.P. and Freed, I.H. (1975) J. Chem. Phys. 79, 489-511.
12 Grinberg, O.Ya., Dubinsky, A.A., Shuvalov, V.F., Oransky, L.G., Kurochkin, V.I. and Lebedev, Ya.S. (1976) Dokl. Akad. Nauk SSSR 230, 885-886.
13 Ondar, M.A., Grinberg, O.Ya., Dubinsky, A.A. and Lebedev, Ya.S. (1984) Khim. Fizika (Russ) 3, 527-536.
14 Grinberg, O.Ya., Dubinsky, A.A., Poluektov, O.G. and Lebedev, Ya.S. (1987) Khim. Fizika (Russ) 6, 1363-1372.
15 Dubinsky, A.A., Grinberg, O.Ya., Kurochkin, V.I., Oransky, L.G., Poluektov, O.G. and Lebedev, Ya.S. (1981) Teoretich. (i) Eksp. Khimija 17, 231-236.
16 Lynch, W.B., Earle, K.A. and Freed, J.H. (1988) Rev. Sci. Instrum. 59, 1345-1351.
17 Krinichnyi, V.I. (1990) Zurn. Prikl. Spektr. 52, 887-905.
18 Buchachenko, A.L. and Wasserman, A.M. (1973) Stable Radicals (Russ), Khimiya, Moskou.
19 Buchachenko, A.L. (1984) Complexes of Radicals and Molecular Oxygen with Organic Molecules (Russ), Nauka, Moskou.
20 Reddoch, A. and Konishi, S. (1979) J. Chem. Phys. 70, 2121-2128.
21 Kivelson, D. (1960) J. Chem. Phys. 33, 1094-1106.
22 McConnell, H.M. (1956) J. Chem. Phys. 25, 709-711.
23 Freed, J.H. and Frankel, G.K. (1963) J. Chem. Phys. 39, 326-348.
24 Johnson, M.E. and Lie, L. (1982) Biochemistry 21, 4459-4463.
25 Galkin, A.A., Grinberg, O.Ya., Dubinsky, A.A., Kabdin, N.I., Krymov, V.N., Kurochkin, V.I., Lebedev, Ya.S., Oransky, L.G. and Shuvalov, V.F. (1977) Prib. i Tekh. Eksp. 4, 284.
26 Kuska, H.A. and Rogers, M.I. (1968) In: E.T. Kaiser and L. Kevan (Eds.), Radical Ions, Intersci. Publ., New York, London, Sydney.
27 Likhtenstein, G.I., Achmedov, Ju.D. and Ivanov, L.V. (1974) Mol. Biol. 8, 48-52.
28 Krinichnyi, V.I., Grinsberg, Ya., Judanova, E.I., Lyubashevskaya, E.V., Antisiferova, L.I., Likhten stein, G.I. and Lebedev, Ya.S. (1987) Biofizika 32, 215-220.
29 Schmidt, P.I. and Kuntz, I.D. (1984) Biochemistry 23, 4261-4265.
30 Krinichnyi, V.I., Grinberg, O.Ya., Bogatyrenko, V.R., Lebedev, Ya.S. and Likhtenstein, S.I. (1985) Biofizika 30, 216-219.
31 Likhtenstein, G.I. (1979) Polynuclear Redox Enzymes, Nauka, Moskou.
32 Krinichnyi, V.I., Grinberg, O.Ya., Yudanova, E.I., Bonn, M.L., Lebedev, Ya.S. and Likhtenstein, G.I. (1987) Biofizika 32, 59-63.
33 Griffith, O. and Jost, P. (1976) In: L. Berliner (Ed.), Spin Labeling. Theory and Application, Vol. 1, Academic Press, New York.
34 Fendler, J.H. and Fendler, E.J. (1975) Catalysis in Micellar and Macromolecular Systems, Academic Press, New York.
35 Belonogova, O.V., Likhtenstein, G.I., Levashov, A.V., Khmelnitsky, Yu.L., KJyachko, N.L. and Martinek, K. (1983) Biokhimiya 48, 379-386.
36 Menger, F.M., Saito, G., Sanzero, S.V. and Dodd, J.R. (1975) J. Am. Chem. Soc. 97, 909-911.
37 Krinichnyi, V.I., Antsiferova, L.T., Lyubashevskaya, E.V., Belonogova, O.V., Grinberg, O.Ya. and Likhtenstein, G.I. (1989) Zurn. Fizich. Khimii 63, 3015-3021.

38 Levashov, A.V., Klyachko, N.L. and Martinek, K. (1981) Bioorg. Khim. 7, 670-679.
39 Kosman, D.J. (1972) J. Mol. Biol. 67, 247-259.
40 Yusupov, l.Kh., Bobodzanov, P.Kh., Marupov, R., Islomov, G., Antsiferova, L.I., Koltover, V.K. and Likhtenstcin, G.I. (1984) Vysokomolekul. Soedin. (A), 26, 369-373.
41 Yershov, B.G. and Klimentov, A.S. (1984) Usphekhi Khimii 53, 2056-2077.
42 Krinichnyi, V.I., Grinberg, O.Ya., Yusupov, l.Kh., Marupov, R., Bobodzanov, P.Kh., Likhtenstein, G.I., and Lebedev, Ya.S. (1986) Biofizika 31, 482-485.
43 Krinichnyi, V.I. and Kostina, N.V. (1989) Intern. Confer. Nitroxyl Radicals (Abstr.), Novosibirsk, 63.
44 Marupov, R., Bobodzanov, P.Kh., Yusupov, l.Kh., Mavlyanov, A.M., Frolov, E.N. and Likhtenstein, G.I. (1979) Biofizika 24, 519-523.
45 Poluectov, O.G., Lyubashevskaya, E.V., Dubinsky, A.A., Antsiferova, L.I. and Lebedev, Ya.S. (1985) Khimich. Fizika 4, 1615-1618.
46 Johnson, M.E. (1978) Biochemistry 17, 1223-1228.
47 Antsiferova, L.I. and Lyubashevskaya, E.V. (1986) The 2 mm Wave Band Spectra Atlas of the Nitroxil Radicals. Izdat. Akad. Nauk/SSSR, Chernogolovka.
48 Hemminga, M.A. (1973) Chem. Phy£ Lipids 32, 323-383.
49 Robinson, B.H. and Dalton, L.R. (1980) J. Chem. Phys. 72, 1312-1323.
50 Lebedev, Ya.S., Antsiferova, L.I., Grinberg, O.Ya., Dubinsky, A.A., Krinichnyi, V.I., Lyubashevskaya, E.V. and Poluektov, O.G. (1985) 2nd Conf. Modern Meth. RFS, DDR-8804, 48-57.
51 Krinichnyi, V.I., Grinberg, O.Ya., Dubinsky, A.A., Livshits, V.A., Bobrov, Yu.A. and Lebedev, Ya.S. (1987) Biofizika 32, 534-535.
52 Ingram, D.I.E. (1969) Biological and Biochemical Application of Electron Spin Resonance. Adam Ailder Ltd., London.
53 Roth, H.K., Keller, F. and Schneider, H. (1984) Hochfrequenz-spektroskopie in der Polymerforschung. Akademie-Verlag, Berlin.
54 Gordy, W. and Kurita, Y. (1960) J. Chem. Phys. 34, 282-288.
55 Copeland, E.S. (1975) J. Magn. Reson. 20, 124-129.
56 Krinichnyi, V.I., Shuvalov, V.F., Grinberg, O.Ya. and Lebedev, Ya.S. (1983) Khimich. Fizika (Russ), 1, 621-627.
57 Dmitruk, A.F., Kholoimova, L.I., Krinichnyi, V.I., Grinberg, O.Ya., Shuvalov, V.F. and Lebedev, Ya.S. (1986) Khimich. Fizika (Russ), 5, 479-483.
58 McCain, D.C. and Palke, W.E. (1975) J. Magn. Reson. 20, 52-66.